The current issue and full text archive of this journal is available at
http://www.emerald-library.com/ft

Received September 1999
Revised September 2000
Accepted September 2000

Heat transfer in a micropolar fluid over a stretching sheet with viscous dissipation and internal heat generation

A.A. Mohammadein
Mathematics Department, Faculty of Science, South Valley University, Aswan, Egypt, and
Rama Subba Reddy Gorla
Mechanical Engineering Department, Cleveland State University, Cleveland, Ohio, USA

Keywords *Heat transfer, Micropolar fluids, Stretching*

Abstract *A boundary layer analysis is presented to study the heat transfer characteristics of a laminar micropolar fluid boundary layer over a linearly stretching, continuous surface. The study considers the effects of viscous dissipation and internal heat generation. Two cases are studied; namely the surface with prescribed uniform surface temperature (PST-case) and the surface with prescribed uniform wall heat flux (PHF-case). The solution for the governing momentum, angular momentum and energy equations are obtained for various values of the material parameters of the micropolar fluid.*

1. Introduction

The laminar boundary layer of a viscous fluid over a moving continuous solid surface is a significant type of flow occurring in several engineering applications. Vajravelu and Rollins (1991) investigated the heat transfer characteristics of a viscoelastic fluid over an impermeable, linearly stretching sheet with power-law surface temperature or surface heat flux. The effects of viscous dissipation and internal heat generation on the heat transfer in the laminar boundary layer of a viscous fluid over a linearly stretching surface with variable wall temperature subject to suction or blowing were considered by Vajravelu and Hadjinicolaou (1993) and Vajravelu (1994).

Eringen (1966) has proposed the theory of micropolar fluids which takes account the inertial characteristics of the substructure particles, which are allowed to undergo rotation. The theory of thermomicropolar fluids has been developed by Eringen (1972). The boundary layer flow of a micropolar fluid over a semi-infinite plate was studied by Ahmadi (1976). Gorla *et al.* (1983) studied the forced convection in a micropolar boundary layer flow on a vertical plate.

In the present paper, we have presented an analysis to study the heat transfer in a micropolar fluid over a stretching sheet in the presence of viscous

The authors are grateful to the reviewers for their useful comments.

dissipation and internal heat generation. Two cases are studied, namely, the uniform surface temperature and uniform surface heat flux boundary conditions. The governing equations were solved numerically. The numerical results are presented for a range of values of the material parameters, the heat source/sink parameters and Eckert number.

2. Flow analysis

Consideration may be given to the problem of a flat porous surface issuing from a very thin slit at $x = 0, y = 0$ and subsequently being stretched, as in a polymer extrusion process (see Figure 1). It is assumed that the speed of a point on the surface is proportional to its distance from the slit. The boundary layer equations for the steady, two-dimensional, incompressible viscous micropolar flow may be written as:

Mass:

$$\frac{\partial u}{\partial x} + \frac{\partial v}{\partial y} = 0, \tag{1}$$

Momentum:

$$u\frac{\partial u}{\partial x} + v\frac{\partial u}{\partial y} = (\nu + \frac{K}{\rho})\frac{\partial^2 u}{\partial y^2} + \frac{K}{\rho}\frac{\partial N}{\partial y} \tag{2}$$

Angular momentum:

$$u\frac{\partial N}{\partial x} + v\frac{\partial N}{\partial y} = \frac{\gamma}{\rho j}\frac{\partial^2 N}{\partial y^2} - \frac{K}{\rho j}(2N + \frac{\partial u}{\partial y}) \tag{3}$$

where u and v are the velocity components in the x and y direction, respectively, N angular velocity, K, ρ, ν, γ and j are the vortex viscosity, the density, the kinematic viscosity, the spin gradient viscosity and the microinertia per unit mass.

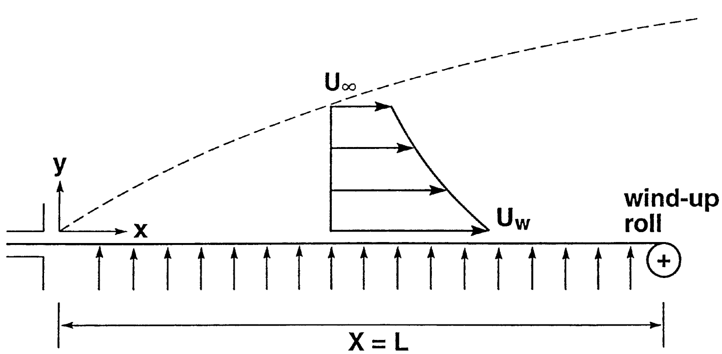

Figure 1.
A sketch of the physical model

The appropriate boundary conditions are given by:

$$u = Bx, \quad v = v_w, \quad N = 0 \ \ at \ \ y = 0 \ \ (B \succ 0), \\ u \to 0, \qquad N \to 0 \qquad as \ \ y \to \infty. \tag{4}$$

Equations (1-3) admit a self-similar solution:

$$u = Bxf'(\eta), \quad v = -\sqrt{B\nu}f(\eta) \\ N = Bx\sqrt{\frac{B}{\nu}}g(\eta) \\ \eta = \sqrt{\frac{B}{\nu}}y \tag{5}$$

where η is the similarity space variable, $f(\eta)$ and $g(\eta)$ are the

Clearly u and v defined in equation (5) satisfy the continuity equation (1). Substituting the transformations (5) in (2-4) we get:

$$(1 + \Delta)f''' + \Delta g' + ff'' - (f')^2 = 0 \tag{6}$$

$$\lambda g'' - \Delta \cdot B_1(2g + f'') - f'g + g'f = 0 \tag{7}$$

and the transformed boundary conditions are:

$$f'(0) = 1, \ \ f(0) = -v_w/\sqrt{B\nu} = f_w, \quad g(0) = 0 \\ f'(\infty) = 0, \quad g(\infty) = 0 \tag{8}$$

In the above equations, a prime denotes differentiation with respect to η, and $B_1 = \nu/jB$, $\lambda = \gamma/\rho j\nu$ and $\Delta = K/\rho\nu$. The case corresponding to $f_w < 0$ implies blowing ($v_w > 0$) and $f_w > 0$ implies suction ($v_w < 0$). In the case of $f_w = 0$, the stretching sheet is impermeable.

The wall shear stress is given by:

$$\tau_w = [(\mu + K)\frac{\partial u}{\partial y} + KN]_{y=0} \\ = \mu Bx\sqrt{\frac{B}{\nu}}(1 + \Delta)f''(0) \tag{9}$$

3. Heat transfer analysis

The boundary layer energy equation with viscous dissipation and internal heat generation or absorption is:

$$\rho C_p(u\frac{\partial T}{\partial x} + v\frac{\partial T}{\partial y}) = k\frac{\partial^2 T}{\partial y^2} + (\mu + K)(\frac{\partial u}{\partial y})^2 + Q(T - T_\infty) \tag{10}$$

where k is the thermal conductivity, C_p is the specific heat, and Q is the volumetric rate of heat generation.

3.1 Prescribed surface temperature (PST-case)

For this case, the boundary conditions are:

$$\begin{aligned} &T = T_w = cons\tan t \quad &at \ \ y = 0, \\ &T \to T_\infty &as \ \ y \to \infty, \end{aligned} \tag{11}$$

Defining the dimensionless temperature by:

$$\theta(\eta) = \frac{(T - T_\infty)}{(T_w - T_\infty)} \tag{12}$$

and using the relations (5), the energy equation (10) and the boundary conditions (11) become:

$$\theta'' + \sigma f \theta' + \sigma\alpha\theta + (1 + \Delta)\sigma E(f'')^2 = 0, \tag{13}$$

$$\begin{aligned} &\theta = 1 \quad &at \ \ \eta = 0, \\ &\theta \to 0 &as \ \eta \to \infty \end{aligned} \tag{14}$$

where:

$\sigma = \mu C_p/k$, the Prandtl number;

$\alpha = Q/B\rho C_p$, the heat source/sink parameter;

$E = B^2L^2/C_pA$, the Eckert number;

$L =$ characteristic length;

$A = (T_w - T_\infty)$

3.2 Prescribed wall heat flux (PHF-case)

For this case, the boundary conditions are:

$$\begin{aligned} &-k(\frac{\partial T}{\partial y}) = q_w = cons\tan t \quad &at \ \ y = 0, \\ &T \to T_\infty &as \ \ y \to \infty. \end{aligned} \tag{15}$$

Defining:

$$T - T_\infty = \frac{D}{k}\sqrt{\frac{\nu}{B}}(\frac{x}{L})^2\phi(\eta), \tag{16}$$

and substituting the relations (5) into (10) and (15), we get

$$\phi'' + \sigma f \phi' - \sigma(2f' - \alpha)\phi + (1 + \Delta)\sigma E(f'')^2 = 0, \tag{17}$$

$$\phi'(0) = -1, \qquad \phi(\infty) = 0, \tag{18}$$

where:

$\sigma = \mu C_p / k$, the Prandtl number;

$\alpha = Q / B \rho C_p$, the heat source/sink parameter;

E = Eckert number.

4. Results and discussion

The governing boundary layer equations for the velocity, microrotation and temperature have been solved on the digital computer using the Runge-Kutta numerical integration procedure in conjunction with shooting techniques. In the numerical solution, a check was made to confirm that smoothness conditions at the edge of the boundary layer were satisfied. An integration step size of $\Delta\eta = 0.01$ and a value of η_∞, the edge of the boundary layer, ranging from 8 to 12 was found to be adequate to satisfy a convergence criterion of 10^{-6} at the boundary layer edge.

Tables I and II contain a summary of numerical results. Table I shows the surface values of velocity gradient and the values of microrotation component. The former is proportional to the friction factor whereas the latter to the wall couple stress. Table II shows the surface values of temperature gradient for PST-case and the surface values of temperature for PHF-case. Here, we have $\sigma = 0.72$, $B_1 = 0.1$, $\lambda = 0.5$ while Δ, α, f_w and E were varied over a range.

Figures 2 and 3 display several dimensionless velocity profiles $f'(\eta)$ and microrotation profiles $g(\eta)$ versus space variable η, for the prescribed surface temperature (PST) case or prescribed wall heat flux (PHF) case, for several values of the dimensionless parameter f_w and Δ when $B_1 = 0.1$, $\lambda = 0.5$ and $\sigma = 0.72$. The results indicate that the boundary layer thickness of velocity and angular velocity fields increases with increasing Δ and decreases with increasing f_w. The microrotation component decreases monotonically to zero at the boundary layer edge. The magnitude of the velocities is smaller for micropolar fluids in comparison with Newtonian fluids. This may be explained by the fact that due to the increased viscosity of micropolar fluids, the velocity is reduced.

Figure 4 displays several dimensionless temperature profiles $\theta(\eta)$ versus space variable η, for the prescribed surface temperature (PST) case, for several values of the dimensionless parameter f_w, α, E and Δ when $B_1 = 0.1$, $\lambda = 0.5$

Table I. Wall values of velocity and microrotation gradients

	$f_w = -0.2$		$f_w = 0.0$		$f_w = 0.2$	
Δ	$-f''(0)$	$g'(0)$	$-f''(0)$	$g'(0)$	$-f''(0)$	$g'(0)$
0.0	0.90500	0	1.00001	0	1.10499	0
0.5	0.74987	0.03833	0.81391	0.04383	0.88344	0.04931
1.5	0.58238	0.08901	0.62136	0.10165	0.66304	0.11473
5.0	0.36334	0.17318	0.37988	0.19607	0.39729	0.22060

△	α	E	$f_w = -0.02$ $-\theta'(0)$	$\phi(0)$	$f_w = 0.0$ $-\theta'(0)$	$\phi(0)$	$f_w = 0.2$ $-\theta'(0)$	$\phi(0)$
0.0	–0.1	0.0	1.07508	0.93016	1.13170	0.88363	1.19261	0.83849
		0.01	1.07294	0.93215	1.12919	0.88585	1.18969	0.84095
		0.5	0.96805	1.02971	1.00606	0.99465	1.04617	0.96128
	0.0	0.0	1.03306	0.96800	1.08862	0.91859	1.14889	0.87041
		0.01	1.03088	0.97011	1.08606	0.92095	1.14591	0.87300
		0.5	0.92380	1.07376	0.96046	1.03632	0.99967	1.00029
	0.1	0.0	0.98586	1.01434	1.04021	0.96134	1.09995	0.90913
		0.01	0.98362	1.01661	1.03759	0.96386	1.09690	0.91191
		0.5	0.87381	1.12800	0.90893	1.08755	0.94737	1.04785
0.5	–0.1	0.0	1.11470	0.89710	1.17800	0.84890	1.24556	0.80285
		0.01	1.11305	0.89858	1.17610	0.85051	1.24339	0.80459
		0.5	1.03253	0.97082	1.08326	0.92932	1.13698	0.89003
	0.0	0.0	1.07706	0.92845	1.13993	0.87725	1.20731	0.82829
		0.01	1.07538	0.93001	1.13800	0.87894	1.20510	0.83012
		0.5	0.99319	1.00632	1.04328	0.96203	1.09664	0.91996
	0.1	0.0	1.03659	0.96470	1.09901	0.90991	1.16627	0.85743
		0.01	1.03488	0.96636	1.09703	0.91171	1.16401	0.85937
		0.5	0.95072	1.04754	1.00014	0.99988	1.05318	0.95440
1.5	–0.1	0.0	1.15552	0.86541	1.22414	0.81690	1.29699	0.77102
		0.01	1.12435	0.86642	1.22282	0.81798	1.29550	0.77217
		0.5	1.09734	0.91576	1.15814	0.87081	1.22253	0.82843
	0.0	0.0	1.12138	0.89176	1.18994	0.84038	1.26290	0.79183
		0.01	1.12019	0.89282	1.18860	0.84151	1.23138	0.79303
		0.5	1.06195	0.94475	1.12256	0.89700	1.18693	0.85199
	0.1	0.0	1.08557	0.92117	1.15410	0.86648	1.22721	0.81485
		0.01	1.08436	0.92229	1.15272	0.86767	1.22566	0.81612
		0.5	1.02473	0.97722	1.08516	0.92621	1.14955	0.87814
5.0	–0.1	0.0	1.20616	0.82908	1.27630	0.78167	1.35651	0.73718
		0.01	1.20553	0.82960	1.27859	0.78223	1.35572	0.73777
		0.5	1.17435	0.85545	1.24379	0.80943	1.31707	0.76626
	0.0	0.0	1.17535	0.85081	1.24865	0.80087	1.32612	0.72408
		0.01	1.17470	0.85136	1.24792	0.80145	1.32531	0.75469
		0.5	1.14277	0.87853	1.21228	0.82999	1.28575	0.78452
	0.1	0.0	1.14354	0.87448	1.21701	0.82168	1.29478	0.77233
		0.01	1.14287	0.87507	1.21627	0.82230	1.29396	0.77297
		0.5	1.11010	0.90372	1.17971	0.85233	1.25340	0.80429

Table II. Wall values of surface temperature gradient (PST-case) and surface temperature (PHF-case)

and $\sigma = 0.72$. Comparing the curves we note that the temperature at a given point (fixed η) decreases with an increase in the micropolar parameter Δ and the same with suction/blowing parameter f_w. This means that the thermal boundary layer thickness decreases with increasing Δ and f_w. It is also seen that the temperature increases with an increase in the heat source/sink parameter α. The same trend occurs with an increase in the frictional heating parameter (Eckert number) E.

The dimensionless wall temperature gradient, $\theta'(0)$, as a function of the micropolar parameter, Δ, for several sets of values of the dimensionless parameters f_w and α when $E = 0.01$ is shown graphically in Table II. The

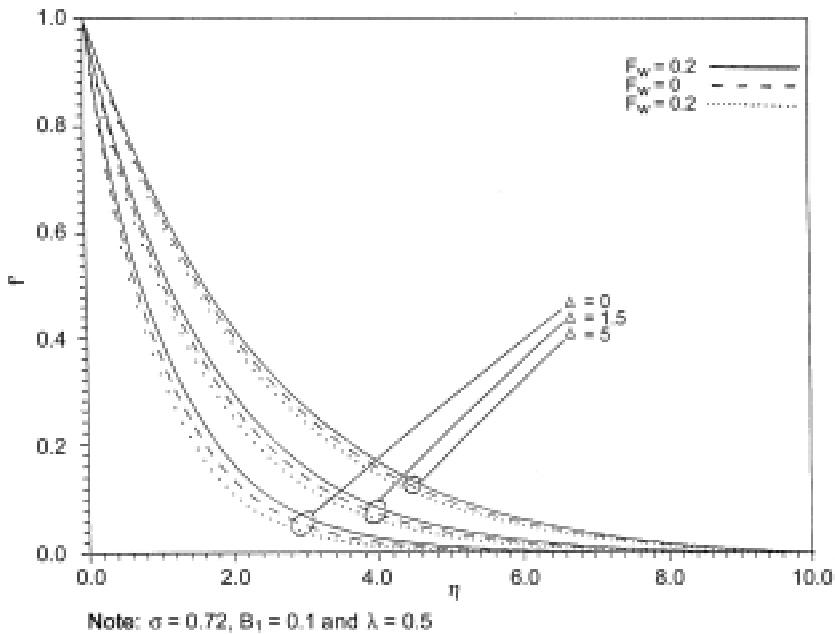

Figure 2.
Velocity profiles (PST or PHF-case) for various values of Δ and f_w

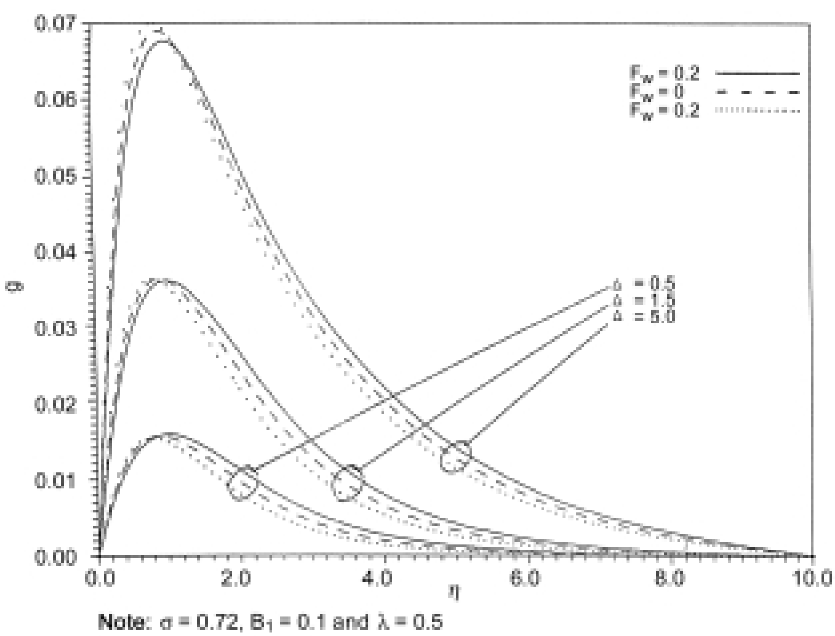

Figure 3.
Microrotation profiles (PST or PHF-case) for various values of Δ and f_w

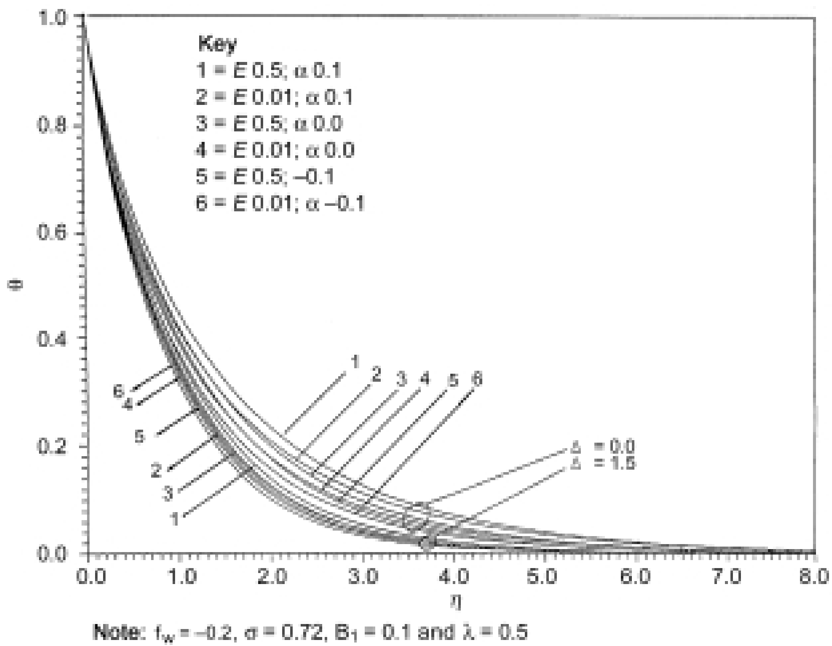

Figure 4.
Temperature profiles (PST-case) for various values of Δ, α and E

magnitude of the wall temperature gradient increases with increasing values of f_w and Δ. The opposite behavior is observed as α increases. Furthermore, the negative values of the wall temperature gradient are indicative that the heat flows from the surface to the ambient fluid.

The behavior of the wall temperature $\phi(0)$ with changes in f_w, α and Δ when $E = 0.01$ is shown in Table II. The wall temperature decreases as Δ increases. Furthermore, it is observed that for fixed Δ, the larger the suction/blowing parameter f_w, the smaller is the wall temperature. In addition, the wall temperature increases as the heat source/sink parameter α increases. Finally, it should be mentioned that for a Newtonian fluid ($\Delta = 0$), the results of the present study reduce to those of Vajravelu and Hadjinicolaou (1993).

The micropolar material parameter Δ is proportional to the spin gradient viscosity of the fluid microstructure. Increasing it results in flow retardation, which in turn decreases the rate of heat transfer convected away from the heated wall. This is clearly seen from the present results. It may be observed from the results that as Δ increases, the magnitude of friction factor and heat transfer rate decrease whereas the gradient of microrotation increases. This indicates that micropolar fluids display drag reduction and reduced heat transfer rates.

5. Concluding remarks

In this paper, we have derived a set of boundary layer equations for the heat transfer characteristics of the laminar boundary layer of a micropolar fluid over a linearly stretching, continuous surface. Consideration is given to uniform surface temperature and uniform surface heat flux boundary conditions subject to suction or blowing in the presence of viscous dissipation and internal heat generation. Numerical solutions are presented for the fluid flow and heat transfer characteristics. The surface friction and heat transfer rate in the case of micropolar fluids are observed to be less than the case of Newtonian fluids.

References

Ahmadi, G. (1976), "Self-similar solution of incompressible micropolar boundary layer flow over a semi-infinite plate", *International Journal of Engineering Science*, Vol. 14, pp. 639-46.

Eringen, A.C. (1966), "Theory of micropolar fluids", *Journal of Mathematics and Mechanics*, Vol. 16, pp. 1-18.

Eringen, A.C. (1972), "Theory of thermomicropolar fluids", *Journal of Mathematical Analysis and Application*, Vol. 38, pp. 488-96.

Gorla, R.S.R., Pender, R. and Eppich, J. (1983), "Heat transfer in micropolar boundary layer over a flat plate", *International Journal of Engineering Science*, Vol. 21, pp. 791-8.

Vajravelu, K. (1994), "Flow and heat transfer in a saturated porous medium over a stretching surface", *Zeitschrift fur Angewandte Mathematik und Mechanik J.*, Vol. 74 No. 12, pp. 605-14.

Vajravelu, K. and Hadjinicolaou, A. (1993), "Heat transfer in a viscous fluid over a stretching sheet with viscous dissipation and internal heat generation", *International Communications in Heat Mass Transfer*, Vol. 20, pp. 417-30.

Vajravelu, K. and Rollins, D. (1991), "Heat transfer characteristics in viscoelastic fluid over a stretching sheet", *Journal of Mathematical Analysis and Applications*, Vol. 158, pp. 241-6.